Supplement of Atmos. Chem. Phys., 23, 10287–10311, 2023
https://doi.org/10.5194/acp-23-10287-2023-supplement

Atmospheric Chemistry and Physics
Open Access
EGU

Supplement of

OH, HO_2, and RO_2 radical chemistry in a rural forest environment: measurements, model comparisons, and evidence of a missing radical sink

Brandon Bottorff et al.

Correspondence to: Brandon Bottorff (brapbott@indiana.edu) and Philip S. Stevens (pstevens@indiana.edu)

Text S1: In order to determine the relative accuracy of the LIF and ECHAMP radical measurements, on July 25th the ECHAMP sampled from the IU calibration source. For this comparison, isoprene was added to the humidified air, producing 50% HO_2 and 50% isoprene-RO_2. Two data points were collected: 1: Calibration source = 335 ppt HO_2 + isoprene RO_2, RH = 33%, ECHAMP measured 326 ppt, 2. Calibration source = 314 ppt HO_2 + isoprene RO_2, RH = 31%, ECHAMP measured 309 ppt.

One reason for this excellent agreement (within 3%) is that the largest source of uncertainty for the calibration gas concentration - the product of the UV lamp actinic flux and the irradiation time ("Ft") - was tied to readings from ECHAMP as it was determined by the measurement of O_3 in the ECHAMP background channel when sampling dry zero air (Kundu et al., 2019). The Licor 6262 H_2O measurements used for the IU calibration source also agreed with the water vapor mixing ratios determined using the ECHAMP RH/T probe within 5%.

Table S1: Measured compounds used as model constraints within RACM and respective measurement sources (CU: University of Colorado, UH: University of Houston, NE: IMT Nord Europe, UM: University of Minnesota, HU: Harvard University, NCAR: National Center for Atmospheric Research, SUNY: University at Albany)

RACM2 input	Grouped compounds	Source	RACM2 input	Grouped compounds	Source
H2	hydrogen	Calc.	NO	nitrous oxide	NCAR
O3	ozone	CU	NO2	nitric oxide	NCAR
CO	carbon monoxide	UH	HONO	nitrous acid	SUNY
SO2	sulfur dioxide	UH	ISO	isoprene	UM
H2O	water vapor	UH	MVK	methylvinylketone	UM
CH4	methane	Calc.	MACR	methacrolein	UM/NE
ETH	ethane	NE	API	monoterpenes	UM
HC3	propane, n-butane, isobutane	NE	BALD	benzaldehyde	UM
			ACD	acetaldehyde	UM
HC5	isopentane, n-pentane, n-heptane, dimethylbutane, 2-methylpentane, 3-methylpentane, n-hexane	NE	ACT	acetone	UM
			HCHO	formaldehyde	HU/NE
			ALD	propanal, butanal	NE
			GLY	glyoxal	NE
HC8	ethyne, nonane	NE	MGLY	methylglyoxal	NE
ETE	ethene	NE	BEN	benzene	UM
OLI	trans-2-butene	NE	TOL	toluene, ethylbenzene, 2-ethyltoluene	UM/NE
OLT	propene, 1-butene	NE			
DIEN	butadiene	NE	XYP/XYM	m,p-xylene	NE
MEK	methylethylketone	NE	XYO	o-xylene	NE

Table S2: Model constraints, their designation within MCM, and respective measurement sources.

MCM Designation	Measured Constraint
University of Houston	
T	temperature
RH	relative humidity
P	pressure
$j(NO_2)$	photolysis rate constant
SO2	sulfur dioxide
CO	carbon monoxide
University of Colorado	
O3	ozone
National Center for Atmospheric Research	
NO	nitric oxide
NO2	nitrogen dioxide
University of Minnesota	
C5H8	isoprene
APINENE	monoterpenes
CH3CHO	acetaldehyde
CH3COCH3	acetone
BENZENE	benzene
CH3OH	methanol
TOLUENE	toluene
MVK	methyl vinyl ketone
MACR	methacrolein
Harvard University	
HCHO	formaldehyde
SUNY	
HONO	nitrous acid
IMT Nord Europe	
HCHO	formaldehyde
C2H2	ethyne
C2H4	ethene
C2H6	ethane
C3H6	propene
C3H8	propane
NC4H10	n-butane
IC4H10	isobutane
BUT1ENE	1-butene
TBUT2ENE	trans-2-butene
C4H6	1,3-butadiene
M22C4	2,2-dimethylbutane
M3PE	3-methylpentane
M2PE	2-methylpentane
NC5H12	n-pentane
IC5H12	isopentane
NC6H14	hexane
NC7H17	n-heptane
NC9H20	nonane
MEK	methyl ethyl ketone
MGLYOX	methylglyoxal
C2H5CHO	propanal
C3H7CHO	butanal
BENZAL	benzaldehyde
EBENZ	ethylbenzene
TM135B	mesitylene
OETHTOL	2-ethyltoluene
OXYL	o-xylene
MXYL	m-xylenes
STYRENE	styrene

Table S3: Summary of measurements (range of daily maximum or maximum diurnal average) of OH, HO_2, XO_2, isoprene, temperature, ozone, and NO_x from previous field campaigns at the PROPHET site.

Campaign (reference)	Dates	[OH] (cm^{-3})	HO_2 (ppt)	XO_2 (ppt)	Isoprene (ppb)	MTs (ppb)	Temp. (C)	O_3 (ppb)	NO_x (ppb)
PROPHET 1997 (Mihele and Hastie, 2003) (Sillman et al., 2002)	Jul. 29–Aug. 14	--------	--------	20-65	~2–6	---	----	~20-80	~0.2–1.8
PROPHET 1998 (Tan et al., 2001)	Aug. 4–14	4×10^6 (Potential interference)[a]	18 (HO_2^*)[b]	--------	2.5	0.04–0.40	28	46	1.1
PROPHET 2008 (Griffith et al., 2013)	Jul. 8–27	3×10^6 (Potential interference)[a]	20 (HO_2^*)[b]	--------	2.3	0.25	24	33	2.1
CABINEX 2009 (Griffith et al. 2013)	Jul. 21–Aug. 9	1.5×10^6 (No observed interference)	18 (HO_2^*)[b]	--------	1.5	0.25	20	35	0.8
PROPHET 2016 (This work)	Jul. 1–31	1.3×10^6 (No observed interference)	14	30	2.9	0.30	24	38	0.8

[a] OH measurements in 1998 and 2008 may have been influenced by unknown interferences similar to Mao et al. (2012), Feiner et al. (2016), and Lew et al. (2020).

[b] For campaigns in 1998, 2008, and 2009 higher concentrations of NO were added to the LIF detection cell, leading to the detection of both HO_2 and a fraction of RO_2 radicals, denoted as HO_2^* ($HO_2^* = HO_2 + \alpha RO_2$, $0<\alpha<1$).

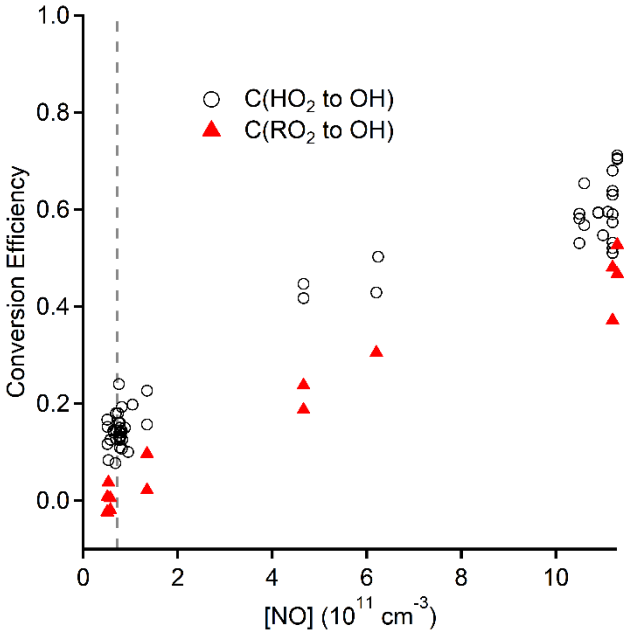

Figure S1: Conversion efficiencies of HO_2 to OH (black open circles) and isoprene RO_2 to OH (red triangles) as a function of the NO concentration inside the sampling cell. The measured values were obtained from calibrations performed before and during the campaign. The vertical dashed line indicates the NO concentration used for HO_2 measurements.

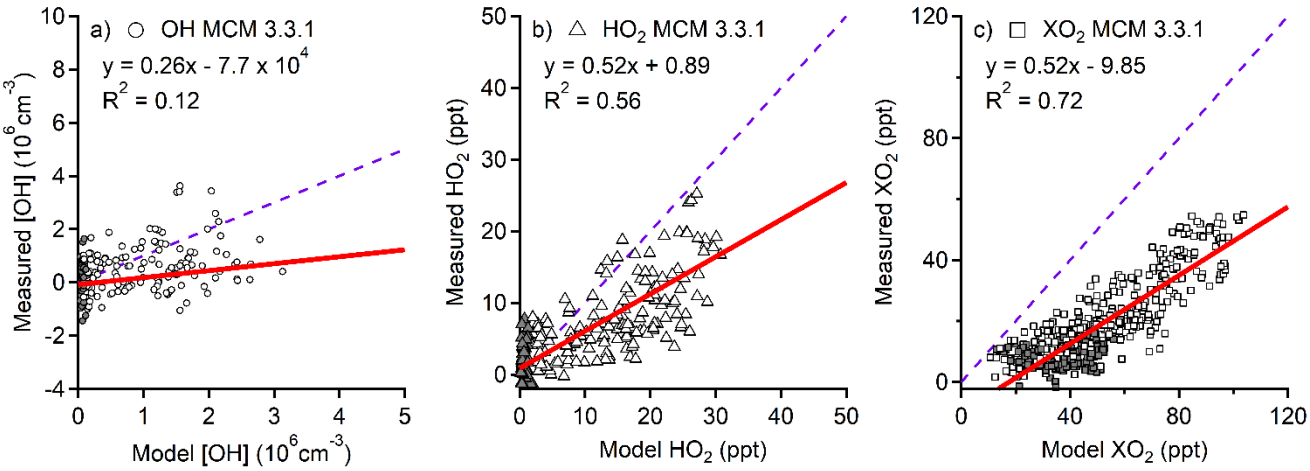

Figure S2: Correlation plots of modeled radical concentrations (MCM v3.3.1) against measurements of a) OH (circles), b) HO_2 (triangles), and c) XO_2 (squares). Filled symbols denote nighttime and open symbols indicate measurements made during the day. The dashed purple line indicates a 1:1 correlation and the red lines show measurement vs. model regressions of the data weighted by both the precision of the measurements and the uncertainty of the model concentrations.

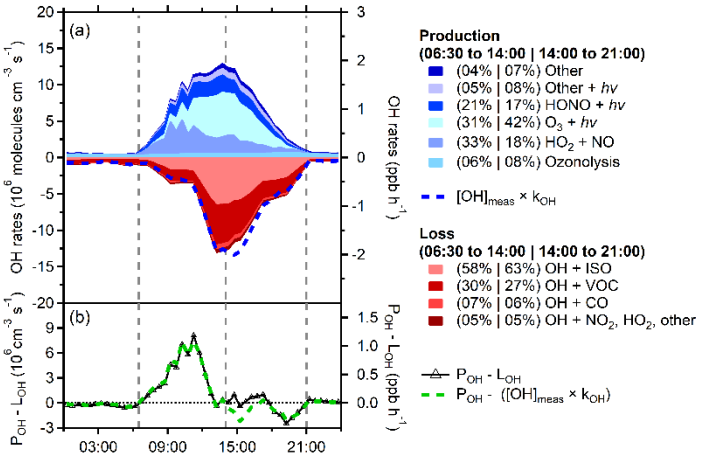

Figure S3: Experimental OH radical budget. In panel (a), shades of blue represent reactions that produce OH, and shades of red represent loss rates, including reactions that propagate to RO_2 or HO_2. Percentages indicate the relative contribution of each respective process in the morning (06:30: to 14:00) and during the evening (14:00 to 21:00) time periods which are indicated by the vertical dashed lines. The blue dashed line represents the total OH loss rate calculated from measured concentrations of OH and the measured OH reactivity. The net rate of production or loss is shown in panel (b).

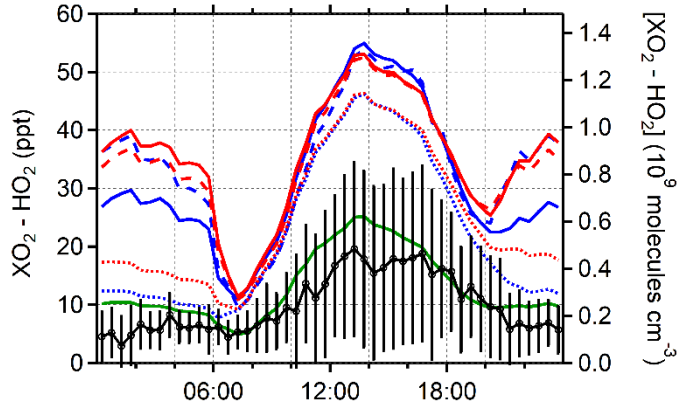

Figure S4: Diurnal average measured (black) and modeled concentrations of RO_2. MCM models are shown in red and RACM2 in blue. The green line represents an additional version of the RACM-ACC model with added sinks for HO_2 and isoprene peroxy radicals. The measured RO_2 mixing ratios were determined by subtracting the measured HO_2 (LIF) from the measured XO_2 (ECHAMP).

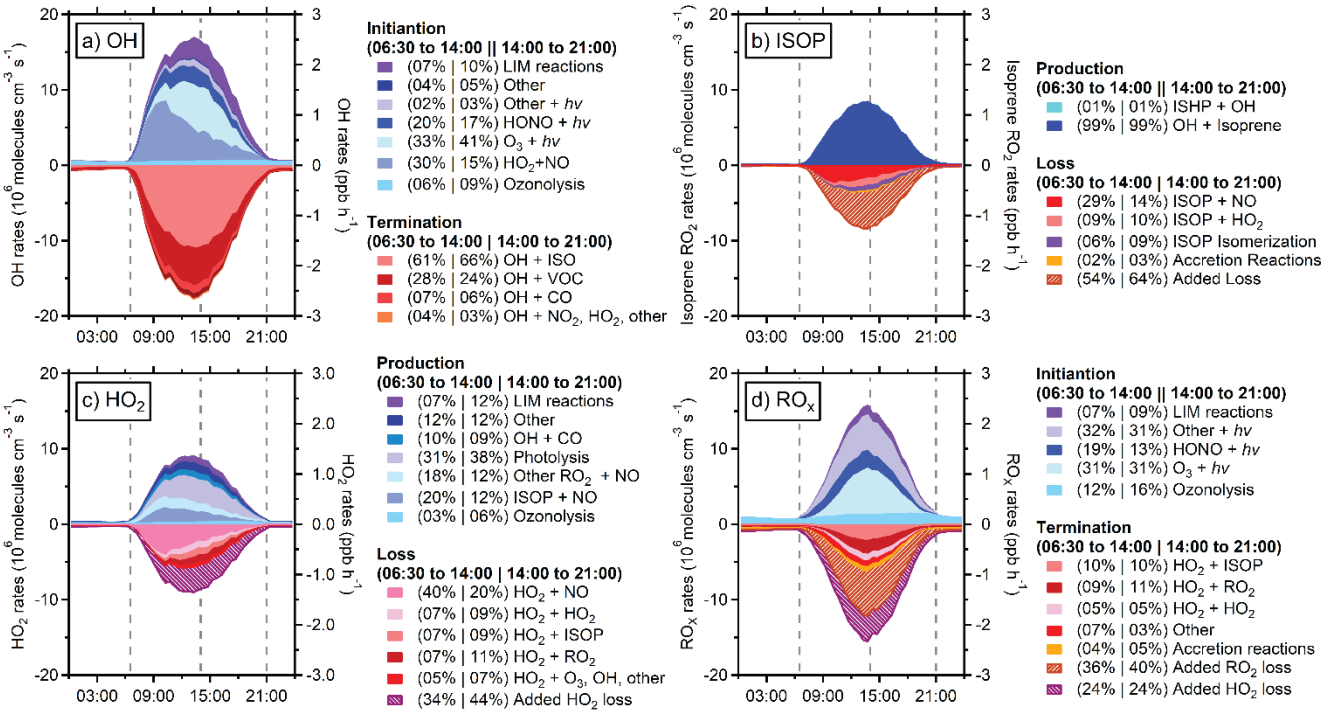

Figure S5: Radical budgets for a) OH, b) HO_2, c) isoprene-RO_2, and d) total RO_x from the RACM-ACC model with added loss mechanisms for HO_2 and isoprene RO_2. Shades of blue represent reactions that produce OH, and shades of red represent loss rates, including reactions that propagate to RO_2 or HO_2. Percentages represent the relative initiation or termination rates of each respective process in the morning (06:30: to 14:00) and during the evening (14:00 to 21:00) which are indicated by the vertical dashed lines.

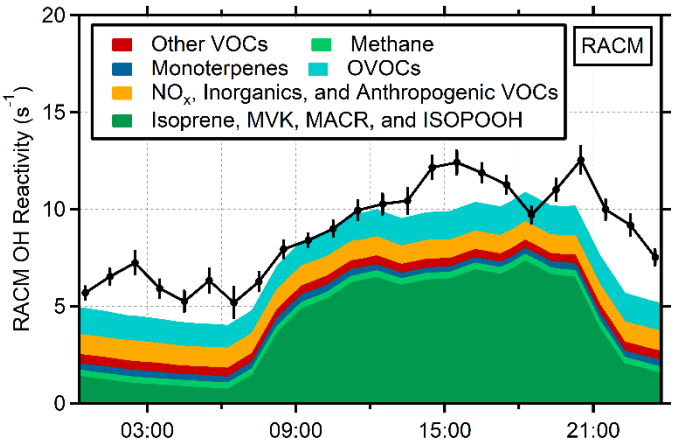

Figure S6: Diurnal average of the measured (IU-TOHLM instrument) and modeled total OH reactivity at the top of the tower during PROPHET-AMOS. Modeled reactivity is largely based on measured species that are used as constraints in the RACM2-LIM1 model.

References

Feiner, P. A., Brune, W. H., Miller, D. O., Zhang, L., Cohen, R. C., Romer, P. S., Goldstein, A. H., Keutsch, F. N., Skog, K. M., Wennberg, P. O., Nguyen, T. B., Teng, A. P., DeGouw, J., Koss, A., Wild, R. J., Brown, S. S., Guenther, A., Edgerton, E., Baumann, K., and Fry, J. L.: Testing Atmospheric Oxidation in an Alabama Forest, J. Atmos. Sci., 73, 4699-4710, https://doi.org/10.1175/JAS-D-16-0044.1, 2016.

Griffith, S. M., Hansen, R. F., Dusanter, S., Stevens, P. S., Alaghmand, M., Bertman, S. B., Carroll, M. A., Erickson, M., Galloway, M., Grossberg, N., Hottle, J., Hou, J., Jobson, B. T., Kammrath, A., Keutsch, F. N., Lefer, B. L., Mielke, L. H., O'Brien, A., Shepson, P. B., Thurlow, M., Wallace, W., Zhang, N., and Zhou, X. L.: OH and HO_2 radical chemistry during PROPHET 2008 and CABINEX 2009 - Part 1: Measurements and model comparison, Atmos. Chem. Phys., 13, 5403-5423, https://doi.org/10.5194/acp-13-5403-2013, 2013.

Kundu, S., Deming, B. L., Lew, M. M., Bottorff, B. P., Rickly, P., Stevens, P. S., Dusanter, S., Sklaveniti, S., Leonardis, T., Locoge, N., and Wood, E. C.: Peroxy radical measurements by ethane – nitric oxide chemical amplification and laser-induced fluorescence during the IRRONIC field campaign in a forest in Indiana, Atmos. Chem. Phys., 19, 9563-9579, https://doi.org/10.5194/acp-19-9563-2019, 2019.

Lew, M. M., Rickly, P. S., Bottorff, B. P., Reidy, E., Sklaveniti, S., Léonardis, T., Locoge, N., Dusanter, S., Kundu, S., Wood, E., and Stevens, P. S.: OH and HO_2 radical chemistry in a midlatitude forest: measurements and model comparisons, Atmos. Chem. Phys., 20, 9209-9230, https://doi.org/10.5194/acp-20-9209-2020, 2020.

Mao, J., Ren, X., Zhang, L., Van Duin, D. M., Cohen, R. C., Park, J. H., Goldstein, A. H., Paulot, F., Beaver, M. R., Crounse, J. D., Wennberg, P. O., DiGangi, J. P., Henry, S. B., Keutsch, F. N., Park, C., Schade, G. W., Wolfe, G. M., Thornton, J. A., and Brune, W. H.: Insights into hydroxyl measurements and atmospheric oxidation in a California forest, Atmos. Chem. Phys., 12, 8009-8020, https://doi.org/10.5194/acp-12-8009-2012, 2012.

Mihele, C. M. and Hastie, D. R.: Radical chemistry at a forested continental site: Results from the PROPHET 1997 campaign, J. Geophys. Res.- Atmos., 108, 4450, https://doi.org/10.1029/2002JD002888, 2003.

Sillman, S., Carroll, M. A., Thornberry, T., Lamb, B. K., Westberg, H., Brune, W. H., Faloona, I., Tan, D., Shepson, P. B., Sumner, A. L., Hastie, D. R., Mihele, C. M., Apel, E. C., Riemer, D. D., and Zika, R. G.: Loss of isoprene and sources of nighttime OH radicals at a rural site in the United States: Results from photochemical models, J. Geophys. Res.- Atmos., 107, ACH 2-1-ACH 2-14, https://doi.org/https://doi.org/10.1029/2001JD000449, 2002.

Tan, D., Faloona, I., Simpas, J. B., Brune, W., Shepson, P. B., Couch, T. L., Sumner, A. L., Carroll, M. A., Thornberry, T., Apel, E., Riemer, D., and Stockwell, W.: HO_x budgets in a deciduous forest: Results from the PROPHET summer 1998 campaign, J. Geophys. Res.- Atmos., 106, 24407-24427, https://doi.org/10.1029/2001JD900016, 2001.